Original Research Article

Paeoniflorin Inhibits Atrial Fibrosis and Atrial Fibrillation in Angiotensin II-Infused Mice Through the PI3K-Akt Pathway

Dose-Response:
An International Journal
October-December 2024:1–13

DOI: 10.1177/15593258241277919
journals.sagepub.com/home/dos
Sage

Yaqiong Ji[1] and Zhongping Ning[2]

Abstract

Objective: The investigation aimed to analyze the effect of Paeoniflorin (PF) on the initiation of atrial fibrosis and atrial fibrillation (AF) induced by angiotensin II (Ang II) and explore its associated underlying mechanism. **Introduction:** PF has anti-inflammatory, immunomodulatory, antioxidant, hepatoprotective, and hypolipidemic properties. However, the protective effect of PF against atrial fibrosis and AF remains unclear. **Methods:** Male C57BL/6 mice aged 8-10 weeks, with 40 individuals, were subjected to subcutaneous infusion of either saline or Ang II at a dosage of 2.0 mg/kg/day. Furthermore, PF at a dosage of 100 mg/kg/day was administered through gavage once daily for 28 days. Morphological, histological, and biochemical examinations were undertaken. AF was elicited through in vivo transesophageal burst pacing. **Results:** PF treatment significantly improved AF in Ang II-infused mice. In addition, PF attenuated cardiac hypertrophy, atrial fibrotic area, atrial apoptosis and oxidative stress in Ang II-induced mice. The effect of PF on the PI3K-Akt pathway reduced the expression of phosphoinositide 3-kinase (p-PI3K) and Phosphorylated Akt (p-Akt) in Ang II-induced mice. **Conclusion:** PF may, therefore, avert Ang II-induced atrial fibrosis and AF by inhibiting the PI3K-Akt pathway.

Keywords

paeoniflorin, angiotensin II, atrial fibrosis, atrial fibrillation, apoptosis

Introduction

Atrial fibrillation (AF) is recognized as a highly prevalent cardiac arrhythmia on a global scale, with considerable morbidity, mortality, and clinical burden.[1] It is defined as an irregular cardiac rhythm resulting from rapid and disordered electrical signals in the atria.[2] With AF being associated with poor health outcomes and significant costs for health care, averting the onset and development of AF is inevitably required. Atrial fibrosis serves as a fundamental factor contributing to cardiac remodeling in AF, where the connective myocardium undergoes redistribution and is substituted by impaired tissue.[3] This characteristic is commonly found in individuals with AF, disrupting the cellular connections of cardiomyocytes through interference with the mechanical conduction of electrical impulses.[4] Consequently, atrial fibrosis stands out as a key element of atrial structural remodeling, which holds significance in the initiation and perpetuation of AF.[5] Recent observations indicate that the renin-angiotensin system (RAS), specifically involving Ang II as the primary mediator, influences the progression of atrial fibrosis.[6] However, Ang II promotes fibrosis in several ways, including boosting Ca^{2+} levels, stimulating fibroblast proliferation and

[1] Department of Cardiology, Shanghai University of Traditional Chinese Medicine, Shanghai, China
[2] Department of Cardiology, Shanghai Pudong New Area Zhoupu Hospital(Shanghai Health Medical College Affiliated Zhoupu Hospital), Shanghai, China

Received 23 April 2024; accepted 5 August 2024

Corresponding Author:
Dr. Zhongping Ning, Department of Cardiology, Shanghai Pudong New Area Zhoupu Hospital (Shanghai Health Medical College Affiliated Zhoupu Hospital), No.1500 Zhou yuan Road, Pudong New District, Shanghai 201318, China.
Email: ningzpsh@163.com

differentiation, and excessive production of reactive oxygen species (ROS).[7] Ang II has, therefore, been frequently employed in studies to persuade atrial fibrosis to understand better the mechanism of atrial remodeling in AF.[8]

The PI3K-Akt pathway is a crucial signaling pathway that plays an important role in cell processes.[9] This pathway is mediated by the phosphorylation of downstream substrates and is named after 2 key genes: PI3K and Akt.[10] Akt is an AGC family protein with three isoforms: Akt1, Akt2, and Akt3. Phosphatidylinositol 3 kinase (PI3K) is a crucial upstream activator of Akt.[11] The primary function of this pathway is to promote metabolism, cell survival, growth, and angiogenesis in response to external signals.[12] However, regulating the PI3K-Akt pathway could be a potential target to inhibit angiotensin II-induced atrial fibrosis and AF.

Paeoniflorin (PF), the principal active compound found in the complete glycoside of paeony, represents a monoterpene glucoside component present in *Paeonia lactiflora* 'Pallas'.[13] The structural formula of PF can be observed in Figure 1A. Various research studies have highlighted the diverse pharmacological properties of PF, including its anti-inflammatory, immunomodulatory, antioxidant, hepatoprotective, and hypolipidemic effects.[14] Several investigations have indicated the potential therapeutic role of PF in conditions such as rheumatoid arthritis, psoriasis, diabetic nephropathy, ulcerative colitis, and ischemic disorders affecting organs like the heart, liver, and brain.[14-19] Recent scientific inquiry has suggested a protective role of PF against liver-related ailments like hepatic ischemia and reperfusion injury, chemically-induced liver damage, cholestasis, liver fibrosis, and non-alcoholic fatty liver disease (NAFLD).[20] Moreover, PF has been shown to mitigate steatosis, inflammation, ballooning degeneration, and necrosis in NAFLD through modulation of the ROCK/NF-B, IRS/Akt/GSK3, and LKB1/AMPK signaling pathways.[20] Nevertheless, the precise impact and underlying mechanism of PF in Ang II-induced atrial fibrosis and AF remain to be elucidated. Therefore, the research aimed to investigate and provide specific information about the protective effects of PF against Ang ll-infused atrial fibrosis and AF and to examine the precise molecular mechanism.

Materials and Methods

Animals and Treatment

Male C57BL/6 mice (8-10 weeks, n = 40) were applied to construct the AF model. Mice were maintained in the SPF

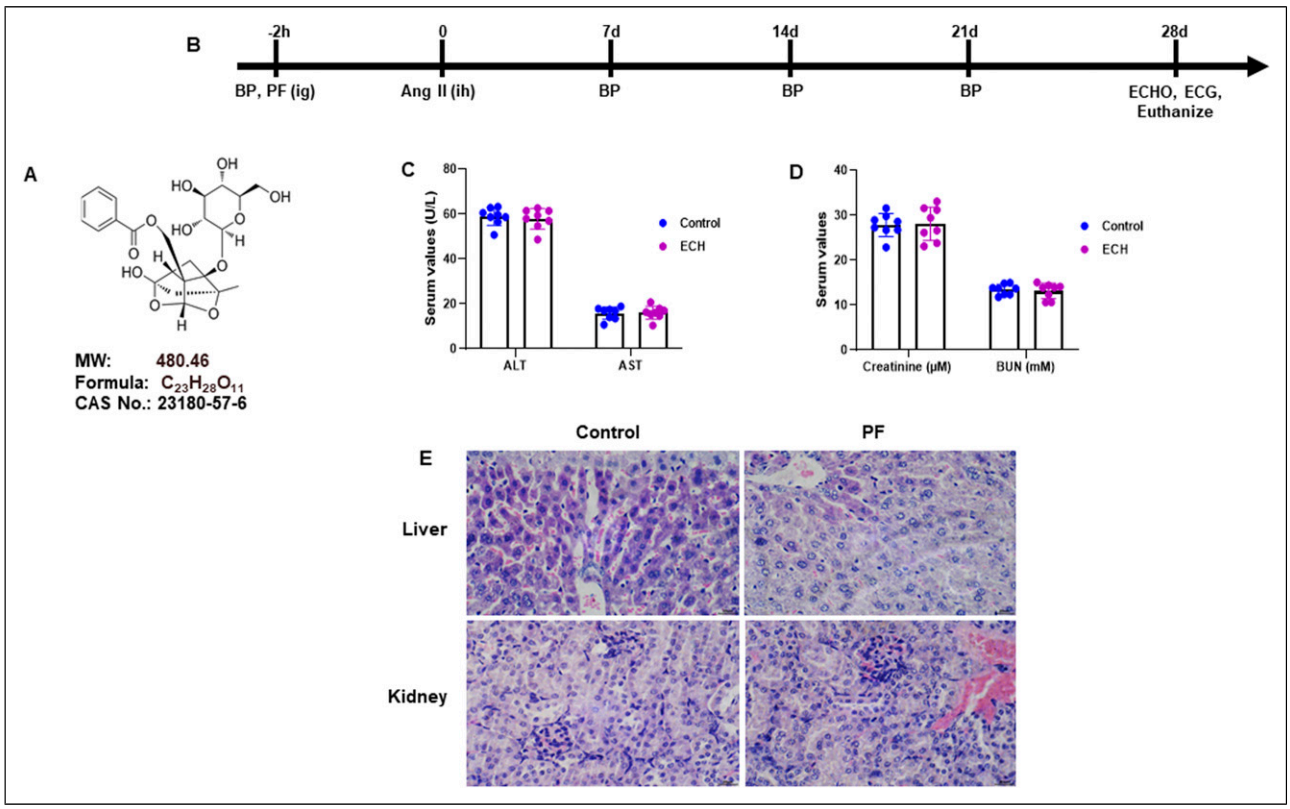

Figure 1. Paeoniflorin has no toxicity to liver and kidney of mice. (A) Chemical Structure of Paeoniflorin. (B) Timeline of interventional procedure of mice. Mice were gavaged with Paeoniflorin (100 mg/kg/day) for 28 consecutively days. (C)-(D) Hepatic and renal function indicators of mice were measured, including ALT, AST, Creatinine and BUN. (E) Hepatic and renal tissues were stained with hematoxylin and eosin (HE) (Magnification 400×). Data are presented as mean ± SD (n = 8 in each group). PF, Paeoniflorin; Ang II, angiotensin II; ALT, alanine transaminase; AST, aspartate transaminase; BUN, blood urea nitrogen.

condition, at 22 ± 2°C temperature and 40% humidity, with a 12 hours light/dark cycle. Using osmotic mini-pumps, mice were subcutaneously infused with either the same volume of saline or angiotensin II (Ang II, 2.0 mg/kg/day, HY-13948, MedChemExpress) for 28 days. Either the same volume of saline or Paeoniflorin (PF, 100 mg/kg/day, HY-N0293, MedChemExpress) was administered through gavage once daily for 28 days. The timeline of interventional procedure of mice is presented in Figure 1B. Our hospital's Animal Care and Use Committee authorised the research. They conducted it in compliance with NIH Publication No. 85-23, updated in 1996, the Guide for the Care and Use of Laboratory Animals.

Animal Grouping and Drug Administration

The mice were categorized into four groups as follows (1) Saline was infused into and gavaged over the eight (8) members of the control group. (2) Saline was infused into the PF group (n = 8) after they were gavaged with PF (100 mg/kg/day). (3) Saline was gavaged, and Ang II (2.0 mg/kg/day) was infused into the Ang II group (n = 8). (4) PF (100 mg/kg/day) was gavaged, and Ang II (2.0 mg/kg/day) was infused into the Ang II + PF group (n = 8). The drug administration lasted for 28 days.

Measurement of Blood Pressure

Systolic blood pressure (SBP) and diastolic blood pressure (DBP) were measured using the tail-cuff system (Softron BP98 A; Softron Tokyo, Japan) on the day prior to Ang II infusion, 7, 14, 21 and 28 days after Ang II infusion. The same person performed all measurements at a fixed time of 15: 00 after the mice were kept quiet for at least 30 min. The O-Cuff sensor and VPR sensor were put on the tail of mice. The SBP and DBP were measured three times to get average values, respectively. The mean arterial pressure (MAP) was assessed from the formula MAP = (SBP + DBP×2)/3.

Echocardiography

The heart function was assessed using the Vevo3100, VisualSonics, Canada, Small Animal Ultrasound Imaging System. M-mode images were obtained to measure the ejection fraction (EF), fractional shortening (FS), left atrial diameter (LAD), left ventricular end-systolic diameter (LVESd), left ventricular end-diastolic diameter (LVEDd), and left ventricular end-diastolic posterior wall thickness (LVPWth).

Electrocardiography

Using the Biological Signal Collection System (MedLab, MadLab-4 C/501H, Beijing, China), mice were anesthetized with an intraperitoneal injection of sodium pentobarbital (50 mg/kg) and surface electrocardiography (ECG) was recorded on day 28 following Ang II infusion. In mice, acetylcholine (Ach) and calcium chloride ($CaCl_2$) saline solution combined to cause AF. Mice were given a 10 mL/kg injection of the Ach-$CaCl_2$ mixture (Ach: 25 μg/mL + $CaCl_2$: 6 mg/mL) via the caudal vein, and 30 minutes later, ECGs were recorded. An irregular, fast atrial rhythm (fibrillatory baseline) with periodic RR intervals lasting at least one second was classified as AF.[21]

Sample Collection

On day 28, after the Ang II infusion, mice were anesthesized, and serum and atrial tissue were collected. The atrial tissue was divided into 2 parts: one part was snap-frozen in liquid nitrogen for RT-qPCR and Western blot, and the other part was fixed in 4% paraformaldehyde for histological analysis.

Measurement of Mice Heart Weight (HW)

After paeoniflorin administration for 28 days, the body weight (BW) of all mice was measured. All mice were sacrificed, and heart tissues and tibias were taken immediately. Meanwhile, the heart weight (HW) and the tibia length (TL) were measured and recorded. Then, the HW/BW and HW/TL ratios were measured.

Biochemical Analysis

Serum was obtained to quantify the biochemical indicators using commercial kits: atrial natriuretic peptide (ANP, E-EL-M0166c, Elabscience, China), brain natriuretic peptide (BNP, E-EL-M0204c, Elabscience, China), cardiac troponin I (cTnI) (SEKM-0153, Solarbio, China), cardiac troponin T (cTnT) (SEKM-0150, Solarbio, China), and alanine transaminase (ALT, C009-2-1, Nanjing Jiancheng Bioengineering Institute, Nanjing, China). Before evaluating the oxidative stress indicators malondialdehyde (MDA, S0131S, Beyotime, Shanghai, China), superoxide dismutase (SOD, S0109, Beyotime), and catalase (CAT, S0051, Beyotime) activities using commercially available kits, the atrial tissues were homogenized in normal cold saline (10% w/v).

Histology

The degrees of liver and kidney injury were evaluated by HE staining. The atrial tissue of mice was stained with HE and Masson's trichrome to assess the morphology and atrial fibrosis. The fibrosis quantification was assessed by the ratio of fibrotic area to normal myocardium (collagen volume fraction).

Tissue Immunofluorescence

The technique of Immunofluorescence was executed following a previously outlined protocol.[22] Frozen sections of

Table 1. The List of Primer Oligonucleotide Sequences Are Used in This Study.

Genes	Forward Primer (5′-3′)	Reverse Primer (5′-3′)
Mouse TGF-β1	AGCAACAATTCCTGGCGTTACCTT	CCTGTATTCCGTCTCCTTGGTTCAG
Mouse CTGF	CCAGACCCAACTATGATGCG	GTGTCCGGATGCACTTTTTG
Mouse MMP-9	CCTGGAACTCACACGACATCTTC	TGGAAACTCACACGCCAGAA
Mouse α-SMA	TCCTGACGCTGAAGTATCCGATA	GGCCACACGAAGCTCGTTAT
Mouse collagen I	GCTCCTCTTAGGGGCCACT	CCACGTCTCACCATTGGGG
Mouse collagen III	TCCCCTGGAATCTGTGAATC	TGAGTCGAATTGGGGAGAAT
Mouse BAX	GCCTCCTCTCCTACTTCGG	AAAAATGCCTTTCCCCTTC
Mouse BCL-2	CTCGTCGCTACCGTCGTGACTTCG	CAGATGCCGGTTCAGGTACTCAGTC
Mouse NOX2	TGGCGATCTCAGCAAAAGGT	ACCTTGGGGCACTTGACAAA
Mouse NOX4	ACCAAATGTTGGGCGATTGTG	GATGAGGCTGCAGTTGAGGT
Mouse GAPDH	ACTCCACTCACGGCAAATTC	TCTCCATGGTGGTGAAGACA

Abbreviation: TGF-β1, transforming growth factor-β1; CTGF, connective tissue growth factor; MMP-9, matrix metalloproteinases-9; α-SMA, α-smooth muscle actin; NOX2, NADPH Oxidase 2; GAPDH: Glyceraldehyde-3-phosphate dehydrogenase.

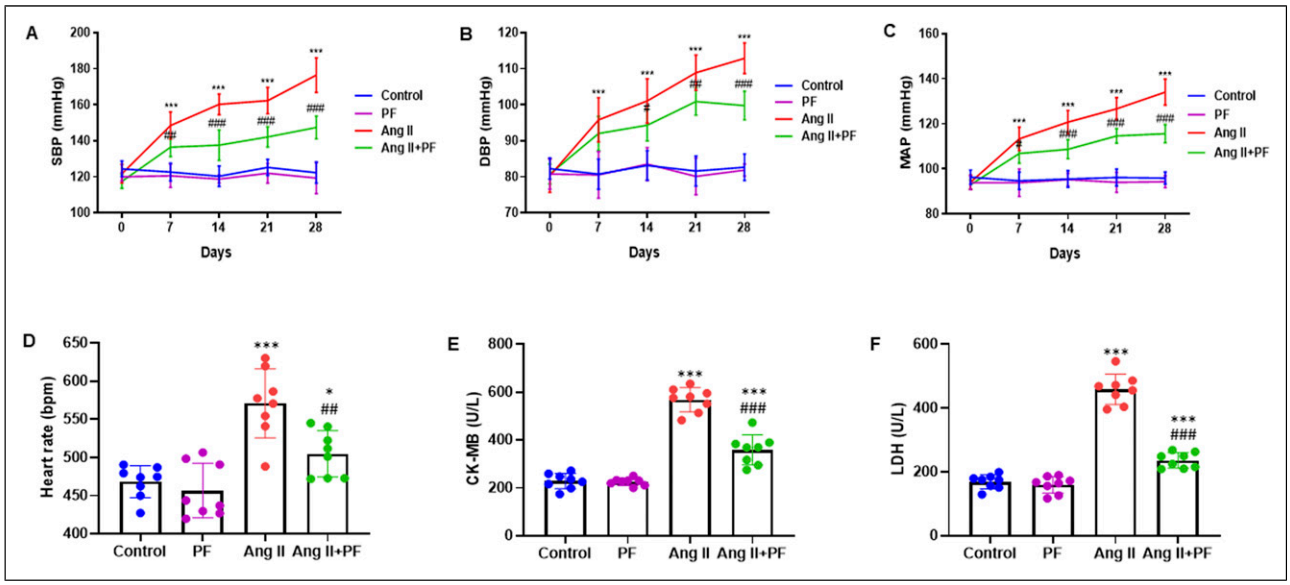

Figure 2. Paeoniflorin regulates physiological parameters in mice. Paeoniflorin was administrated by gavage (100 mg/kg/day) in mice 2 h before subcutaneous infusion of Ang II (2.0 mg/kg/day) for 28 d. Blood pressure were measured every 7 days using the tail-cuff method. Paeoniflorin reduced the (A) SBP, (B) DBP, (C) MAP and (D) heart rate of Ang II-infused mice. The serum levels of (E) CK-MB and (F) LDH were detected to evaluate myocardial injury. Data are presented as mean ± SD (n = 8 in each group). One-way ANOVA with Tuckey's test was used for analysis. *$P < 0.05$, ***$P < 0.001$ vs Control group; ##$P < 0.01$, ###$P < 0.001$ vs Ang II group. SBP, systolic blood pressure; DBP, diastolic blood pressure; MAP, mean arterial pressure; CK-MB, creatine kinase-MB; LDH, lactate dehydrogenase.

murine atrial tissue were procured for analysis. Subsequent to three washes with phosphate-buffered saline (PBS), terminal deoxynucleotidyl transferase dUTP nick end labeling (TUNEL, C1086, Beyotime), Vimentin (ab92547, Abcam, UK), α-smooth muscle actin (α-SMA, ab7817, Abcam, UK), and dihydroergotamine (DHE, S0063, Beyotime) were administered. The specimens were then stained with 4′,6-diamidino-2-phenylindole (DAPI) and scrutinized using an inverted microscope (IX51, Olympus, Japan). The procedures involving TUNEL, Vimentin, α-SMA, and DHE were conducted as per the guidelines provided by the respective manufacturers.

Quantitative Reverse Transcription Polymerase Chain Reaction (RT-qPCR)

TRizol (Invitrogen, USA) was employed to isolate total RNA from cardiac fibroblasts. Subsequently, a process of reverse transcription was undertaken to generate complementary DNA

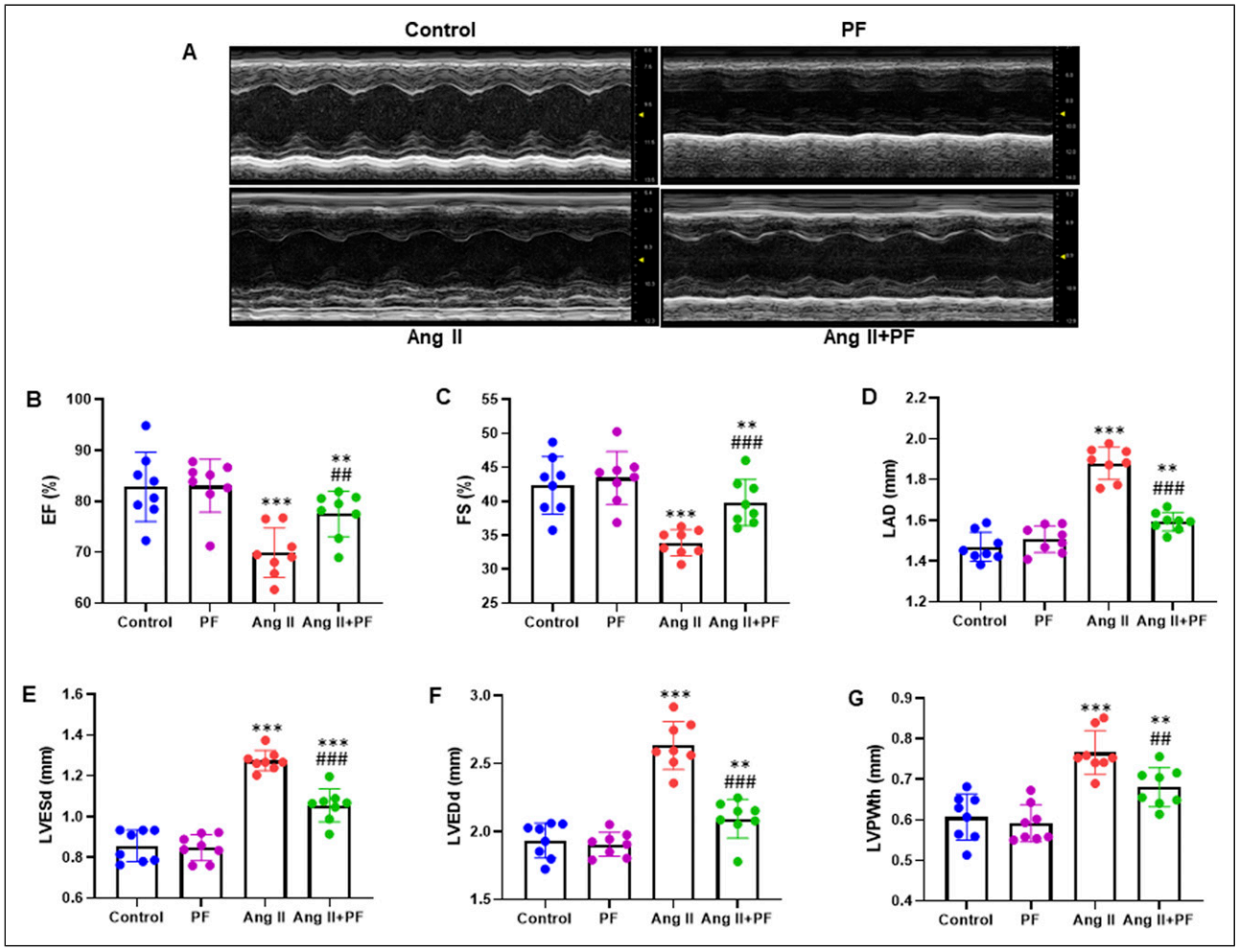

Figure 3. Echocardiographic parameters in mice. (A) Representative M-mode echocardiography images from mice infused with Ang II (2.0 mg/kg/day) and/or gavaged with Paeoniflorin (100 mg/kg/day). Analysis of cardiac functional parameters: (B) ejection fraction (EF); (C) fractional shortening (FS); (D) left atrial diameter (LAD); (E) left ventricular end systolic diameter (LVESd), (F) left ventricular end diastolic diameter (LVEDd); and (G) left ventricular end-diastolic posterior wall thickness (LVPWth). Data are presented as mean ± SD (n = 8 in each group). $^{**}P < 0.01$, $^{***}P < 0.001$ vs Control group; $\#\#P < 0.01$, $\#\#\#P < 0.001$ vs Ang II group.

(cDNA) from the aforementioned total RNA. To conduct amplification of the mRNA through Real-Time Quantitative PCR (RT-qPCR), employment of SYBR Green reagent (TaKaRa, Japan) took place within an ABI Prism 7700 Real-Time PCR apparatus (Applied Biosystems, USA). The calculation of relative gene expression, utilizing the $2^{-\Delta\Delta Ct}$ formula, involved the normalization of the internal control, GADPH.[23] The primers for Mouse TGF-β1, Mouse CTGF, Mouse MMP-9, Mouse α-SMA, Mouse Collagen I, Mouse Collagen III, Mouse BAX, Mouse BCL-2, Mouse NOX2, Mouse NOX4, and Mouse GAPDH were designed by the NCBI Primer-Blast Tool (https://www.ncbi.nlm.nih. gov/tools/primer-blast/), which is listed in Table 1.

Western Blotting

The protein specimens were gathered subsequent to the cell lysis process carried out with RIPA lysis buffer from Beyotime Biotechnology in Shanghai, China. Utilizing a BCA kit by Beyotime, the determination of protein concentration was conducted, followed by the addition of an equal volume of protein (40 μg per well), which was then combined with a loading buffer from Beyotime. Subsequently, the mixture underwent denaturation in a boiling-water bath for a duration of 3 minutes. Electrophoresis commenced once bromphenol blue had traversed the separation gel, with a duration of 30 minutes at 80 V and 1 to 2 hours at 120 V. The proteins were subsequently placed onto membranes in an ice-bath at 300 mA for 60 minutes. After rinsing the membranes for 1~2 minutes with washing solution, they were inactivated for 1 hour at room temperature or sealed overnight at 4°C. The membranes received treatment with the primary antibodies against p-PI3K (p85, Tyr458) (1:400, ab278545, rabbit monoclonal, Abcam), t-PI3K (1:500, ab302958, rabbit monoclonal,

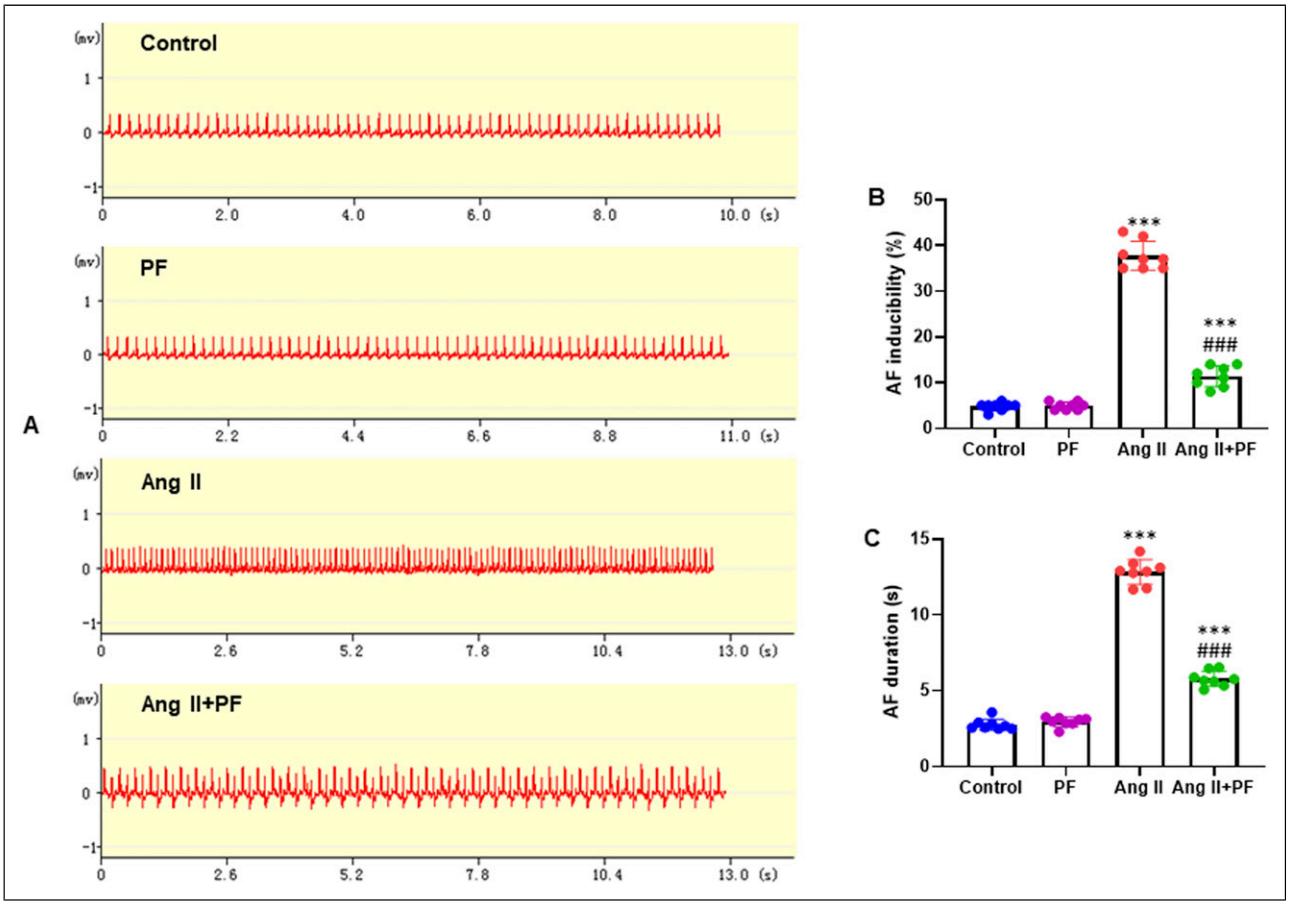

Figure 4. Paeoniflorin reduces atrial fibrillation (AF) inducibility and AF duration of mice. (A) Representative atrial electrogram recordings. Mice were injected the mixture of acetylcholine (Ach) and calcium chloride ($CaCl_2$) through caudal vein. After 30 min, the ECGs were recorded. (B) Percentage of successful AF inducibility. (C) Average AF duration. Data are presented as mean ± SD (n = 8 in each group). ***$P < 0.001$ vs Control group; ###$P < 0.001$ vs Ang II group.

Abcam), p-Akt (Ser473) (1:400, ab81283, rabbit monoclonal, Abcam), and t-Akt (1:400, ab8805, rabbit polyclonal, Abcam) on a shaking table for 1 hour at room temperature. The membranes underwent a series of washing steps using a washing solution thrice within ten minutes before and after 1 hour of exposure to the secondary antibody at ambient temperature. Upon introduction into the development solution, visualization was carried out using a chemiluminescence imaging analysis apparatus (Gel Doc XR, Bio-rad).

Statistical Analysis

All data were presented as the mean value accompanied by the standard deviation (SD) derived from at least three independent experiments. Statistical analyses have been conducted using SPSS 20.0 (SPSS, Chicago, IL, USA) or GraphPad Prism 9.0 software. The differences between several groups were examined using one-way ANOVA and the post hoc Tukey test. AF incidence between various groups was analyzed using Fisher's exact test. Statistical significance has been deemed as a P value of <0.05.

Results

Preliminary Evaluation of the Safety and Physiological Features in Mice

To investigate the possible impact on safety and physiological characteristics in mice after PF administration, mice were administered through gavage once a day for 28 days with PF (100 mg/kg/day). Following 28 days of oral administration through gavage of PF (100 mg/kg/day), an assessment was conducted on the systemic toxicity of PF in vivo. The parameters of hepatic and renal function in mice were scrutinized, encompassing ALT, aspartate aminotransferase (AST), Creatinine, and blood urea nitrogen (BUN). The findings indicated the absence of any detrimental impacts on the hepatic and renal systems compared to the control group treated with saline and the

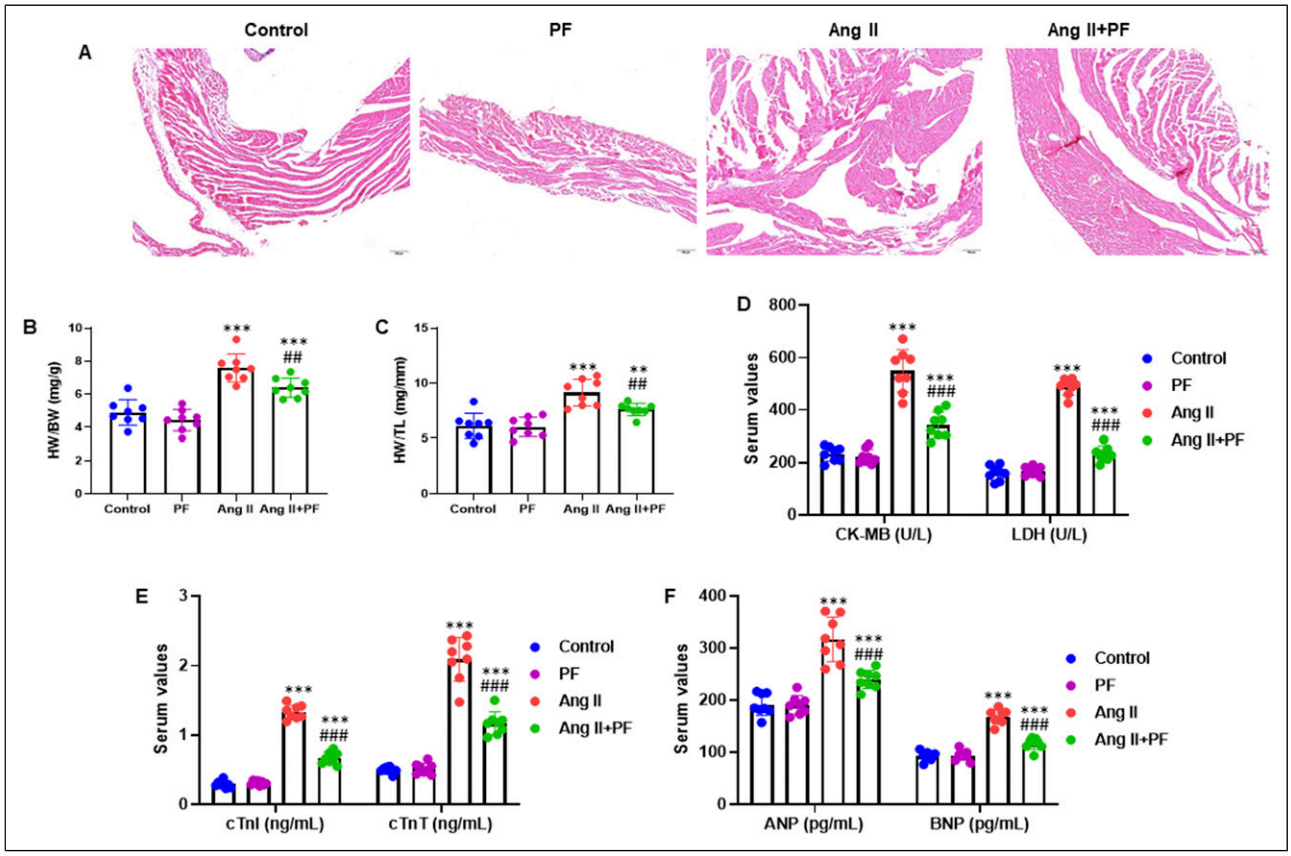

Figure 5. Paeoniflorin suppressed Ang II-induced cardiac hypertrophy and injury in vivo. (A) Heart cross-sections were stained with HE to analyze hypertrophic growth (Magnification 200×). (B)-(C) The HW/BW and HW/TL ratios in mice of four groups. The serum levels of (D) CK-MB (U/L), LDH (U/L), (E) cTnI (ng/mL), cTnT (ng/mL), (F) ANP (pg/mL) and BNP (pg/mL) were measured by ELISA. Data are presented as mean ± SD (n = 8 in each group). $^{**}P < 0.01$, $^{***}P < 0.001$ vs Control group; $^{\#\#\#}P < 0.001$ vs Ang II group. HW, heart weight; BW, body weight; TL, tibia length; CK-MB, creatine kinase isoenzyme MB; LDH, lactate dehydrogenase; cTnI, cardiac troponin I; cTnT, cardiac troponin T; ANP, atrial natriuretic peptide; BNP, brain natriuretic peptide.

mice infused with Ang II (Figure 1C and D). Furthermore, the staining results with Hematoxylin and Eosin (H&E) also exhibited no adverse effects on the liver and kidney (Figure 1E).

To investigate physiological features, mice were given PF (100 mg/kg/day) by gavage 2 hours before receiving Ang II (2.0 mg/kg/day) subcutaneously for a period of 28 days. The findings demonstrated that in Ang II-infused mice, PF decreased heart rate, MAP, DBP, and SBP (Figure 2A-D). In addition, mice had lower serum concentrations of lactate dehydrogenase (LDH) and creatine kinase myocardial band (CK-MB) (Figure 2E and F).

Echocardiographic Features and the Impact of PF on Atrial Fibrillation (AF) in Mice

To investigate the potential impact of the echocardiographic characteristics and the effect of PF on atrial fibrillation (AF) in mice, we infused mice with Ang II (2.0 mg/kg/day) and/or gavaged with PF (100 mg/kg/day). Echocardiography on day 28 showed that Ang II infusion increased LAD in mice, which was attenuated after PF treatment (Figure 3A and D). PF potentially increased the rate of EF and FS (Figure 3B and C). In addition, PF's reduction in the enhancement of LVESd, LVEDd, and LVPWth induced by Ang II, compared to mice treated with Ang II alone. However, PF partially restored the LVESd, LVEDd, and LVPWth levels in the Ang II + PF group than in the control group (Figure 3E-G).

We also studied how PE affected the susceptibility to AF. For 28 days, mice were gavaged with 100 mg/kg/day of PF or infused with Ang II at a 2.0 mg/kg/day dose. The ECG was recorded using transesophageal fast atrial pacing. The AF mice clearly demonstrated typical AF attacks (Figure 4(A)). However, we examined the inducibility and duration of AF in Ang II-infused mice treated with or without PF. The inducibility of AF was low in control mice but significantly elevated after Ang II injection. PF therapy significantly decreased Ang II-induced AF inducibility, whereas PF alone had little effect in saline-treated mice (Figure 4(B)). PF also significantly

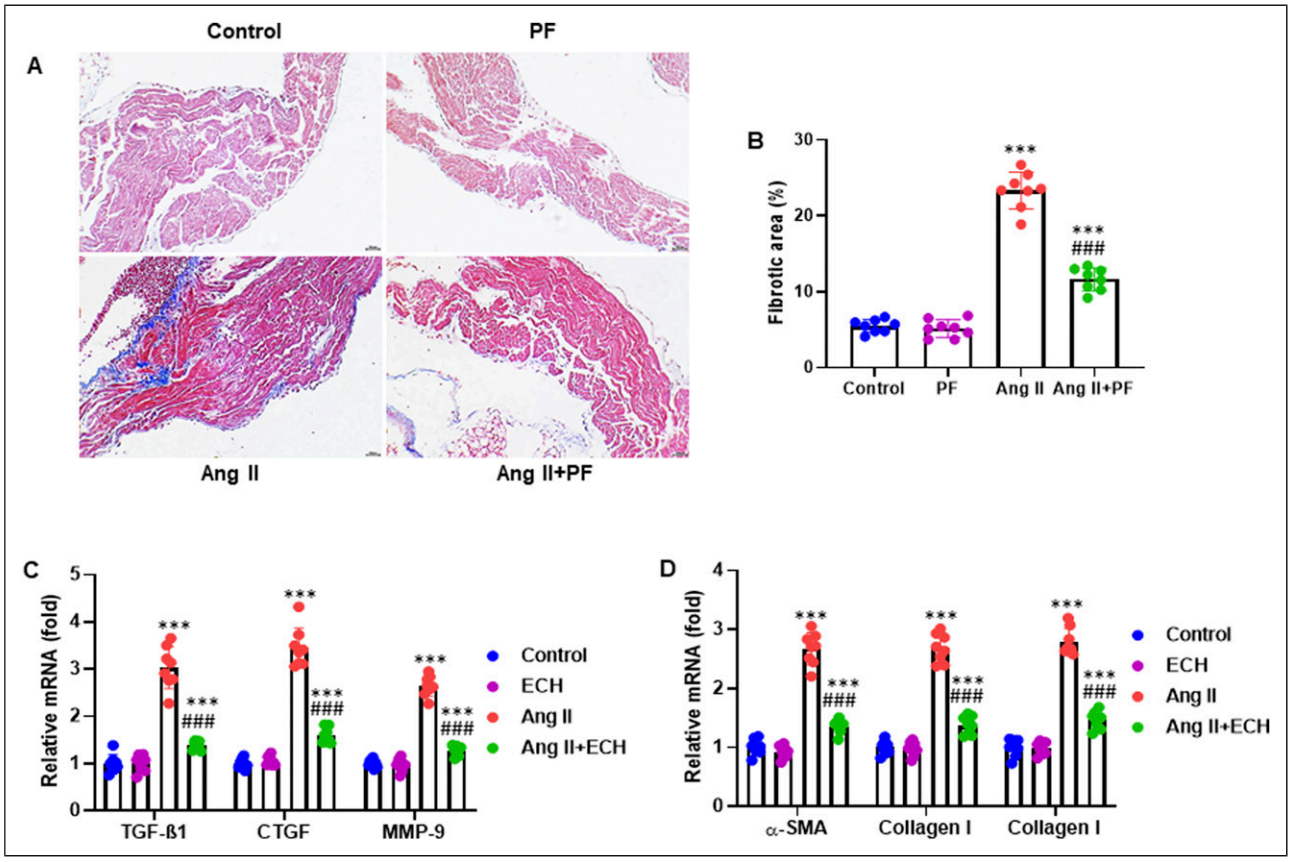

Figure 6. Paeoniflorin suppresses Ang II-induced atrial fibrosis. (A) Atrial tissues were stained with Masson trichrome, the blue area represents the fibrosis, and representative images are shown (Magnification 200×). (B) Quantification of the fibrotic area. RT-qPCR was performed to measure the mRNA expression of (C) TGF-β1, CTGF, MMP-9, and (D) α-SMA, Collagen I and Collagen III. Data are presented as mean ± SD (n = 8 in each group). ***$P < 0.001$ vs control group; ###$P < 0.001$ vs Ang II group. TGF-β1, transforming growth factor-β1; CTGF, connective tissue growth factor; MMP-9, matrix metalloproteinases-9; α-SMA, α-smooth muscle actin.

decreased the average length of AF in Ang II-treated mice, whereas PF therapy alone had little impact on AF duration (Figure 4(C)). However, the inducibility and duration of AF in Ang II-infused mice were partially recovered in the Ang II + PF group than in the control group (Figure 4).

PF Attenuated Ang II-Induced Cardiac Hypertrophy, Injury and Atrial Fibrosis in Vivo

To examine the possible impact of PF in regulating Ang II-infused cardiac hypertrophy, injury and atrial fibrosis, mice were induced with Ang II with or without PF (100 mg/kg/day) for 28 days. Ang II significantly increased hypertrophic growth, while PF remarkably attenuated this effect (Figure 5(A)). In addition, PF markedly reduced the ratio of HW/BW, HW/TL, and the serum levels of CK-MB and LDH were decreased significantly (Figure 5B-D). ELISA measured the serum levels of cTnI, cTnT, ANP, and BNP. The results showed that PF potentially attenuated the serum levels of cTnI, cTnT, ANP, and BNP (Figure 5E and F).

Next, we looked at how PF affected atrial fibrosis, which is a defining feature of atrial remodeling. Ang II markedly increased the atrial fibrotic area, but this effect was remarkably attenuated by PF (Figure 6Aand B). Several fibrotic markers, such as transforming growth factor-β1 (TGF-β1), connective tissue growth factor (CTGF), matrix metalloproteinases-9 (MMP-9), α-SMA, Collagen I, and Collagen III, were measured for their mRNA expression using real-time quantitative polymerase chain reaction (RT-qPCR). The findings showed that TGF-β1, CTGF, MMP-9, α-SMA, Collagen I, and Collagen III were all markedly inhibited by PF (Figure 6C and D).

PF Attenuates Ang II-Induced Atrial Apoptosis and Oxidative Stress

To evaluate the influence of PF on the apoptosis of atrial tissue, TUNEL staining was performed. Ang II infusion showed a noticeable rise in TUNEL + cells (green fluorescence), but this

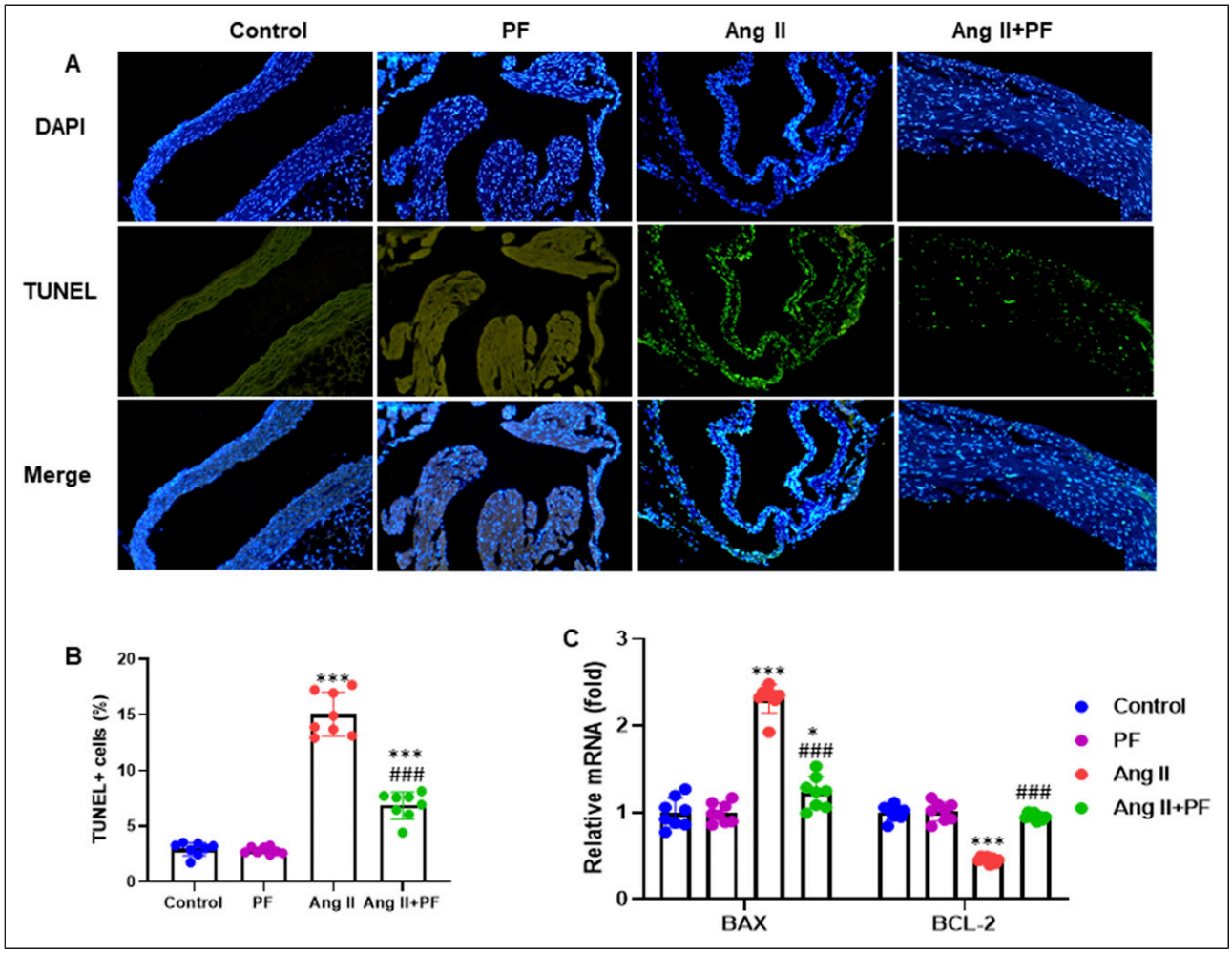

Figure 7. Paeoniflorin reduces atrial apoptosis in mice after Ang II infusion. (A) Atria tissue apoptosis was evaluated by TUNEL staining, and representative images are shown (Magnification 200×). (B) Quantification of the percentage of TUNEL positive cells in atrial tissues. (C) RT-qPCR analyses of the mRNA expression levels of BAX and BCL-2. GAPDH as an internal control. Data are presented as mean ± SD (n = 8 in each group). *$P < 0.05$, ***$P < 0.001$ vs control group; ###$P < 0.001$ vs Ang II group.

increase was diminished in the mice treated with PF (Figure 7A and B). RT-qPCR analyses showed that PF markedly inhibited the mRNA expression levels of BAX and BCL-2 (Figure 7C).

Furthermore, PF treatment reduced the increase in atrial superoxide formation (DHE staining) caused by Ang II infusion (Figure 8A and B). The atrial tissue lysate was used to identify important oxidative stress biomarkers, such as SOD, CAT, and MDA. Increased MDA content and decreased SOD and CAT activity were observed following Ang II infusion, while these changes were all reversed by PF treatment (Figure 8C-E). Meanwhile, RT-qPCR was used to determine the expression of NOX2 and NOX4 genes. The PF treatment dramatically decreased the mRNA expression of NOX2 and NOX4 in mice compared to mice receiving Ang II infusion alone (Figure 8F). However, the atrial apoptosis rate and oxidative stress in Ang II-infused mice were partially restored in the Ang II + PF group than in the control group (Figure 8).

PF regulates the PI3K-Akt pathway in the atrial tissue of Ang II-induced mice

The protein levels of key components of the PI3K-Akt pathway were measured using Western blot. The results indicated that PF markedly inhibited the expression of phosphoinositide 3-kinase (p-PI3K) and Phosphorylated Akt (p-Akt) (Figure 9A). In addition, the quantification analysis of protein bands showed the consistent expression patterns of the western blot analysis (Figure 9B). Protein expression was normalized to total proteins of PI3K and Akt, respectively.

Discussion

There is increasing evidence that PF shows a variety of pharmacological activities. Particularly, PF exhibits anti-inflammatory, antioxidant, anti-arteriosclerotic, recovering cardiac function and reducing cardiac remodeling.[24] Our study demonstrated that PF

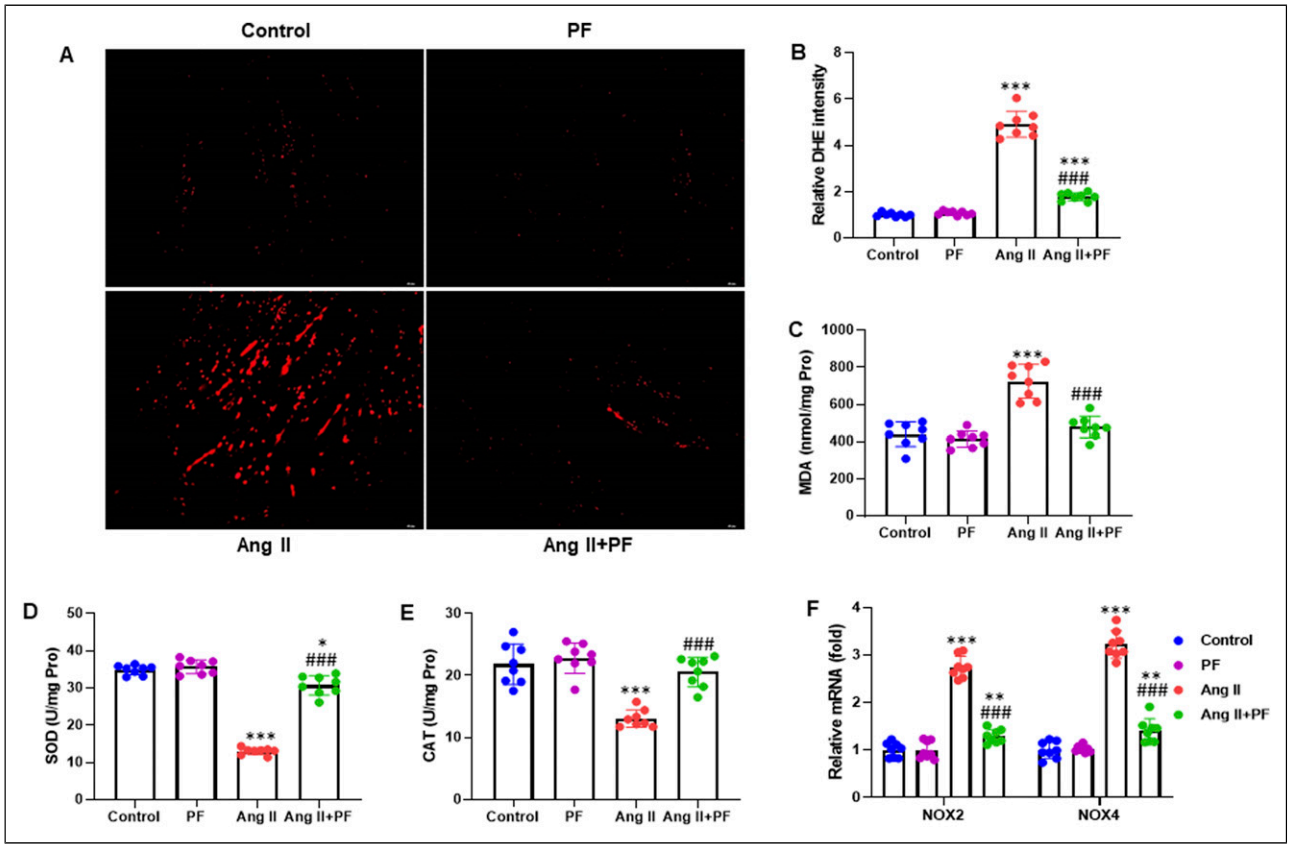

Figure 8. Paeoniflorin suppresses oxidative stress in atrial tissue of mice with Ang II infusion. (A) Atria tissue was stained with DHE, and representative images are shown (Magnification 200×). (B) Quantification of relative DHE intensity. The atrial lysate were analyzed for (C) MDA, (D) SOD and (E) CAT. (F) RT-qPCR was carried out to determine the mRNA expression of NOX2 and NOX4. GAPDH serves as an internal control. Data are presented as mean ± SD (n = 8 in each group). *$P < 0.05$, **$P < 0.01$, ***$P < 0.001$ vs control group; ###$P < 0.001$ vs Ang II group. DHE, dihydroethidium; MDA, malondialdehyde; SOD, superoxide dismutase; CAT, catalase.

had no adverse effects on hepatic or renal tissues and that there were no significant changes in SBP, DBP, MAP, or heart rate. PF significantly attenuated Ang II-infused AF, cardiac hypertrophy, cardiac injury, atrial fibrosis, apoptosis and oxidative stress. In addition, PF significantly reduced the expression of p-PI3K and p-Akt. Therefore, the pharmacological agent PF may exhibit a protective influence against atrial fibrosis induced by Ang II and the subsequent development of AF in mice models.

To evaluate the possible effect on mice safety and physiological features following PF treatment, mice were treated with PF (100 mg/kg/day) via gavage once a day for 28 days. The in vivo systemic toxicity of PF (100 mg/kg/day) was investigated after 28 days of administration via gavage. No adverse effects of PF on the hepatic and renal were observed (Figure 1C-E). For 28 days, mice were gavaged with PF (100 mg/kg/day) 2 hours before subcutaneous infusion of Ang II (2.0 mg/kg/day). The results demonstrated that PF decreased Ang II-infused mice's SBP, DBP, MAP, and heart rate (Figure 2A-D). Furthermore, blood CK-MB and LDH levels were reduced in mice (Figure 2E and F). Moreover, PF treatment significantly improved the rate of EF and FS while inhibiting the increase of LVESd, LVEDd, and LVPWth in Ang II-induced mice. Though PF markedly regulated the echocardiographic features in Ang II + PF group, it could be partially restored as in the control group (Figure 3).

Several criteria are implicated in developing and maintaining AF complications.[25] Atrial fibrosis is the predominant etiology of structural alterations observed in patients with AF and is the underlying structural substrate responsible for its recurrence. Atrial fibrosis progression in the left atrial (LA) contributes to developing focal activities and re-entries, establishing and maintaining AF.[26] Myocardial fibrosis is a common feature observed in both experimental models and individuals with AF.[27] A recent study reported that PE might protect against myocardial ischemia damage, and calcitonin signaling may be implicated in developing AF in mice.[28] Our observation demonstrated that typical AF attacks were seen in AF mice (Figure 4A). PF treatment dramatically reduced Ang II-induced AF inducibility, but PF alone had no impact in saline-treated mice (Figure 4B). PF also significantly decreased the average length of AF in Ang II-treated mice, but PF treatment alone did not affect AF duration (Figure 4C).

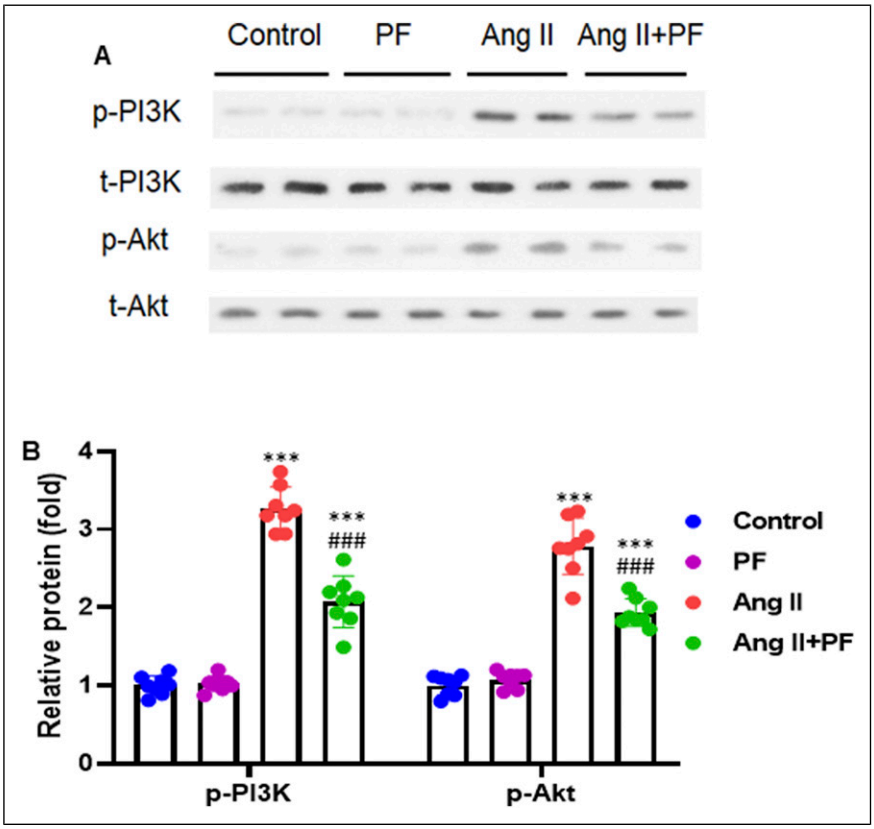

Figure 9. Paeoniflorin regulates PI3K-Akt pathway in atrial tissue of Ang II-treated mice. (A) Representative bands of Western blot results in atrial tissue of mice. (B) Quantification of protein bands for p-PI3K (p85, Tyr458) and p-Akt (Ser473). Protein expression was normalized to the total proteins of PI3K and Akt, respectively. Data are presented as mean ± SD (n = 8 in each group). ***$P < 0.001$ vs control group; ###$P < 0.001$ vs Ang II group.

Though PF significantly inhibited the inducibility and duration of AF in the Ang II + PF group, it could be partially recovered as in the control group (Figure 4).

Pathological cardiac hypertrophy, including hypertension, is strongly connected to the mortality of heart failure patients. Patients with high blood pressure, myocardial infarction, or other cardiovascular diseases might successfully prevent heart failure by suppressing cardiac hypertrophy early.[29] A recent study has shown that increased ROS and apoptosis could contribute to the cardiac hypertrophy produced by several stimulations, including AngII and phenylephrine.[30,31] The development of reactive oxygen species (ROS) and cellular antioxidant capabilities are considered to be discrepancies, resulting in oxidative stress.[32] However, our study showed that Ang II significantly increased hypertrophic growth, while PF remarkably attenuated this effect (Figures 5 and 6). In addition, PF markedly attenuated the Ang II-induced atrial apoptosis and oxidative stress (Figures 7 and 8). This observation is consistent with a recently reported study.[29]

The PI3K-Akt pathway is a pivotal signaling cascade that plays a significant role in cellular processes.[9] This pathway operates through the phosphorylation of downstream substrates and is denoted by the names of 2 pivotal genes, PI3K and Akt.[10] Akt, belonging to the AGC family of proteins, comprises three isoforms: Akt1, Akt2, and Akt3. Acting as a critical upstream stimulator of Akt, Phosphatidylinositol 3 kinase (PI3K) plays a crucial role in this pathway.[11] The principal function of this pathway is to facilitate metabolism, cellular survival, proliferation, and angiogenesis in reaction to external stimuli.[12] However, our study showed that PF significantly inhibiting the expression of p-PI3K and p-Akt (Figure 9).

Our study has several limitations. Firstly, we did not perform a power calculation to estimate the necessary sample size for the study. In the future, we will conduct a power calculation to determine the appropriate sample size. Additionally, we did not assess the efficacy of PF in a dose-dependent manner. This will be evaluated in future research. Furthermore, the results of our study have not been validated in preclinical or clinical settings. The obtained results will be validated in both preclinical and clinical contexts. Lastly, further investigation is required to identify the causative mechanism underlying the protective effects of PF against Ang II-induced atrial fibrosis and AF. Despite these limitations, our study provides significant evidence of the protective effects of PF against atrial fibrosis and AF.

Conclusion

Our accumulating data suggested that PF might be protected against Ang II-infused atrial fibrosis and AF by down-regulating the PI3K-Akt pathway. These findings are needed to be validated in preclinical and clinical settings in the future.

Author contributions

Yaqiong Ji: Conceived and designed the experiments, performed the experiments, analyzed and interpreted the data, and wrote the paper. Zhongping Ning: Conceived and designed the experiments and contributed reagents, materials, analysis tools or data.

Declaration of conflicting interests

The author(s) declared no potential conflicts of interest with respect to the research, authorship, and/or publication of this article.

Funding

The author(s) disclosed receipt of the following financial support for the research, authorship, and/or publication of this article: This study was supported by (1) Key Discipline Group Construction Project of Shanghai Pudong New Area Health Commission (PWZxq2022-11). (2) A prospective cohort study project on the epidemiological investigation and graded diagnosis and treatment mode of atrial fibrillation in Pudong New Area, Shanghai (PKJ2021-Y33). (3) Shanghai Pudong New Area Health Commission Clinical Summit Discipline Construction Project (PWYgf2021-04).

Ethical Statement

Ethics Approval and Consent to Participate

This study was approved (**ZPSH-2019-4**) by Shanghai Pudong New Area Zhoupu Hospital (Zhoupu Hospital affiliated to Shanghai Medical College of Health) Ethics Committee. The authors envisaged all standard protocols in accordance with the 1964 Declaration of Helsinki. All methods carried out in this study were in accordance with ARRIVE guidelines.

ORCID iD

Zhongping Ning https://orcid.org/0000-0001-5851-1223

Data Availability Statement

Due to confidential issues, the datasets generated and/or analyzed during the current work are not publicly available but are available from the corresponding author upon reasonable request.

References

1. Dai H, Zhang Q, Much AA, et al. Global, regional, and national prevalence, incidence, mortality, and risk factors for atrial fibrillation, 1990-2017: results from the global burden of disease study 2017. *Eur Heart J Qual Care Clin Outcomes*. 2021;7(6):574-582.
2. Brundel B, Ai X, Hills MT, Kuipers MF, Lip GY, de Groot NMS. Atrial fibrillation. *Nat Rev Dis Prim*. 2022;8(1):21.
3. Nattel S. Molecular and cellular mechanisms of atrial fibrosis in atrial fibrillation. *JACC Clin Electrophysiol*. 2017;3(5):425-435.
4. Reese-Petersen AL, Olesen MS, Karsdal MA, Svendsen JH, Genovese F. Atrial fibrillation and cardiac fibrosis: a review on the potential of extracellular matrix proteins as biomarkers. *Matrix Biol*. 2020;91-92:188-203.
5. Pellman J, Sheikh F. Atrial fibrillation: mechanisms, therapeutics, and future directions. *Compr Physiol*. 2015;5(2):649-665.
6. Li J, Wang S, Zhang YL, et al. Immunoproteasome subunit β5i promotes Ang II (angiotensin II)-Induced atrial fibrillation by targeting ATRAP (Ang II type I receptor-associated protein) degradation in mice. *Hypertension*. 2019;73(1):92-101.
7. Li CY, Zhang JR, Hu WN, Li SN. Atrial fibrosis underlying atrial fibrillation (Review). *Int J Mol Med*. 2021;47(3):9.
8. Xiao Z, Reddy DPK, Xue C, et al. Profiling of miR-205/P4HA3 following angiotensin II-induced atrial fibrosis: implications for atrial fibrillation. *Front Cardiovasc Med*. 2021;8:609300.
9. Janku F, Yap TA, Meric-Bernstam F. Targeting the PI3K pathway in cancer: are we making headway? *Nat Rev Clin Oncol*. 2018;15:273-291.
10. Chen M, Choi S, Wen T, et al. A p53-phosphoinositide signalosome regulates nuclear AKT activation. *Nat Cell Biol*. 2022;24:1099-1113.
11. Hoxhaj G, Manning BD. The PI3K-AKT network at the interface of oncogenic signalling and cancer metabolism. *Nat Rev Cancer*. 2020;20:74-88.
12. Alzahrani AS. PI3K/Akt/mTOR inhibitors in cancer: at the bench and bedside. *Semin Cancer Biol*. 2019;59:125-132.
13. Wang A, Gong Y, Pei Z, Jiang L, Xia L, Wu Y. Paeoniflorin ameliorates diabetic liver injury by targeting the TXNIP-mediated NLRP3 inflammasome in db/db mice. *Int Immunopharm*. 2022;109:108792.
14. Zhang L, Wei W. Anti-inflammatory and immunoregulatory effects of paeoniflorin and total glucosides of paeony. *Pharmacol Ther*. 2020;207:107452.
15. Zhai W, Ma Z, Wang W, Song L, Yi J. Paeoniflorin inhibits Rho kinase activation in joint synovial tissues of rats with collagen-induced rheumatoid arthritis. *Biomed Pharmacother*. 2018;106:255-259.
16. Gu P, Zhu L, Liu Y, Zhang L, Liu J, Shen H. Protective effects of paeoniflorin on TNBS-induced ulcerative colitis through inhibiting NF-kappaB pathway and apoptosis in mice. *Int Immunopharm*. 2017;50:152-160.
17. Yu J, Xiao Z, Zhao R, Lu C, Zhang Y. Paeoniflorin suppressed IL-22 via p38 MAPK pathway and exerts anti-psoriatic effect. *Life Sci*. 2017;180:17-22.
18. Li Y, Qiao J, Wang B, Bai M, Shen J, Cheng Y. Paeoniflorin ameliorates Fructose-Induced insulin resistance and hepatic steatosis by activating LKB1/AMPK and AKT pathways. *Nutrients*. 2018;10(8):1024.

19. Wen J, Xu B, Sun Y, et al. Paeoniflorin protects against intestinal ischemia/reperfusion by activating LKB1/AMPK and promoting autophagy. *Pharmacol Res*. 2019;146:104308.
20. Ma X, Zhang W, Jiang Y, Wen J, Wei S, Zhao Y. Paeoniflorin, a natural product with multiple targets in liver Diseases-A mini review. *Front Pharmacol*. 2020;11:531.
21. Zou T, Chen Q, Chen C, et al. Moricizine prevents atrial fibrillation by late sodium current inhibition in atrial myocytes. *J Thorac Dis*. 2022;14(6):2187-2200.
22. Li L, Hou X, Xu R, Liu C, Tu M. Research review on the pharmacological effects of astragaloside IV. *Fundam Clin Pharmacol*. 2017;31:17-36.
23. Pfaffl MW. A new mathematical model for relative quantification in real-time RT-PCR. *Nucleic Acids Res*. 2001;29: e45.
24. Li X, Sun C, Zhang J, et al. Protective effects of paeoniflorin on cardiovascular diseases: a pharmacological and mechanistic overview. *Front Pharmacol*. 2023;14:1122969.
25. January CT, Wann LS, Alpert JS, et al. 2014 AHA/ACC/HRS guideline for the management of patients with atrial fibrillation: a report of the American College of Cardiology/American Heart Association task force on practice guidelines and the Heart Rhythm Society. *Circulation*. 2014;130: 199-267.
26. Nattel S, Harada M. Atrial remodeling and atrial fibrillation: recent advances and translational perspectives. *J Am Coll Cardiol*. 2014;63:2335-2345.
27. Burstein B, Nattel S. Atrial fibrosis: mechanisms and clinical relevance in atrial fibrillation. *J Am Coll Cardiol*. 2008;51: 802-809.
28. Han F, Zhou D, Yin X, et al. Paeoniflorin protects diabetic mice against myocardial ischemic injury via the transient receptor potential vanilloid 1/calcitonin gene-related peptide pathway. *Cell Biosci*. 2016;6:37.
29. Ren S, Wang Y, Zhang Y, et al. Paeoniflorin alleviates AngII-induced cardiac hypertrophy in H9c2 cells by regulating oxidative stress and Nrf2 signaling pathway. *Biomed Pharmacother*. 2023;165:115253.
30. Samman Tahhan A, Sandesara PB, Hayek SS, et al. Association between oxidative stress and atrial fibrillation. *Heart Rhythm*. 2017;14:1849-1855.
31. An D, Zeng Q, Zhang P, et al. Alpha-ketoglutarate ameliorates pressure overload-induced chronic cardiac dysfunction in mice. *Redox Biol*. 2021;46:102088.
32. Ramachandra CJA, Cong S, Chan X, Yap EP, Yu F, Hausenloy DJ. Oxidative stress in cardiac hypertrophy: from molecular mechanisms to novel therapeutic targets. *Free Radic Biol Med*. 2021;166:297-312.